Supporting Information

Cation-defect-induced self-reduction towards efficient mechanoluminescence in Mn²⁺-activated perovskite

Yao Xiao[a,#], Puxian Xiong[a,#,], Shuai Zhang[a,f,#], Yongsheng Sun[a], Na Yan[a], Zhiduo Wang[a], Qianyi Chen[a], Peishan Shao[a], Mikhail G. Brik[b,c,d,e], Shi Ye[a], Dongdan Chen[a,*] and Zhongmin Yang[a]*

a. School of Materials Science and Engineering, School of Physics and Optoelectronics, State Key Laboratory of Luminescent Materials and Devices, Institute of Optical Communication Materials, Guangdong Engineering Technology Research and Development Center of Special Optical Fiber Materials and Devices, Guangdong Provincial Key Laboratory of Fiber Laser Materials and Applied Techniques, South China University of Technology.

b. School of Optoelectronic Engineering & CQUPT-BUL Innovation Institute, Chongqing University of Posts and Telecommunications, Chongqing, China.

c. Institute of Physics, University of Tartu, Tartu, Estonia.

d. Faculty of Science and Technology, Jan Długosz University, Częstochowa, Poland.

e. Academy of Romanian Scientists, Bucharest, Romania.

f. Condensed Matter and Interfaces, Debye Institute for Nanomaterials Science, Utrecht University, 3508 TA Utrecht, The Netherlands.

*Corresponding author.

E-mail:

P.X. Xiong: xiongpuxian@scut.edu.cn;

D.D. Chen: ddchen@scut.edu.cn;

Equation S1[1]

$$D_q = \frac{1}{6} Z e^2 \frac{r^4}{R^5} \tag{1}$$

Where D_q is the crystal field strength, Z is valence of the anion, e is electronic charge number, R is bond length, and r is the average value of the 3d electron coordinate.

Equation S2[2]

$$[F(R_\infty)h\mu)]^n = K(h\mu - E_g) \tag{2}$$

Where $F(R_\infty) = (1-R_\infty)^2/(2R_\infty)$ originates from the Kubelka-Munk function, R is reflectance (%), $n = 2$ for direct-gap semiconductor material MGO host confirmed by the DFT calculation[3], $h\mu$ is the photon energy, K is a constant and E_g is the bandgap value. The E_g values can be estimated by extrapolating the linear region of $[F(R_\infty) h\mu]^2 = 0$ to the abscissa $(h\mu)$.

Equation S3[4]

$$R_c = 2[\frac{3V}{4\pi X_c N}]^{\frac{1}{3}} \tag{3}$$

Where V is volume of the unit cell, X_c is critical concentration, and N is the number of available sites per unit cell that Mn^{2+} ion can occupy. According to $V = 902.627$ Å^3, $X_c = 0.025$, and $N = 6$.

Equation S4[5]

$$\frac{I}{x} = K[1 + \beta(x)^{\frac{\theta}{3}}]^{-1} \tag{4}$$

Where I is PL intensity, x is the concentration of doped ion, K and β are the constants for each type of interaction in a given host lattice, and θ is the index of electric multipole corresponded to the dipole-dipole ($\theta = 6$), dipole-quadrupole ($\theta = 8$), and quadrupole-quadrupole ($\theta = 10$), respectively.

Equation S5

Equation **S6**

$$I(t) = I_0 + A_1 \exp\left(\frac{-t}{\tau_1}\right) + A_2 \exp\left(\frac{-t}{\tau_2}\right) \tag{5}$$

$$\tau^* = \frac{A_1\tau_1^2 + A_2\tau_2^2}{A_1\tau_1 + A_2\tau_2} \tag{6}$$

2

Where $I(t)$ is fluorescence intensity, A_1 and A_2 are constants, t is time, and τ_1 and τ_2 are short decay and long decay component, respectively, τ^* is average fluorescence lifetimes.

Table S1 Rietveld refined crystallographic parameters of the $M_{1-x}GOM_x$ (x = 0.0%, 1.0%, 1.5%, 2.0%, 2.5%, 3.0%, 3.5% and 4.0%).

Formula	x=0.0 %	x=1.0 %	x=1.5 %	x=2.0 %	x=2.5 %	x=3.0 %	x=3.5 %	x=4.0 %
Crystal system	Orthorho mbic	Orthorho mbic	Orthorho mbic	Orthorho mbic	Orthorho mbic	Orthorho mbic	Orthorho mbic	Orthorho mbic
Space group	*Pb*ca (61)	*Pb*ca (61)	*Pb*ca (61)	*Pb*ca (61)	*Pb*ca (61)	*Pb*ca (61)	*Pb*ca (61)	*Pb*ca (61)
a (Å)	18.8126 00	18.8166 07	18.8190 16	18.8266 96	18.8289 76	18.8239 75	18.8276 81	18.8302 44
b (Å)	8.95590 0	8.95804 3	8.95931 5	8.96308 0	8.96411 0	8.96097 8	8.96364 4	8.96486 8
c (Å)	5.34340 0	5.34432 8	5.34541 4	5.34787 7	5.34893 8	5.34645 5	5.34798 1	5.34890 0
α=β=γ (°)	90	90	90	90	90	90	90	90
volume (Å^3)	900.276	900.840	901.266	902.428	902.820	901.847	902.550	902.951
Z	16	16	16	16	16	16	16	16
Density (g/cm^3)	4.276	4.273	4.271	4.266	4.264	4.269	4.265	4.263
R$_{wp}$ (%)	8.64	11.35	10.96	10.77	11.43	11.39	11.64	11.12
R$_p$ (%)	7.22	8.96	8.70	8.56	9.06	9.01	9.16	8.89
χ^2	1.762	1.973	1.786	1.842	1.744	2.061	2.264	2.041

Table S2 Different atomic site occupancy and select interatomic distances of $M_{0.975}GOM_{0.25}$.

Element	x	y	z	Occupancy	Bond type	Bond length (Å)
Mg1	0.12289	0.65224	0.85428	0.984	Mg1-O1	2.17336
Mn1	0.12289	0.65224	0.85428	0.016	Mg1-O2	2.02703
Mg2	0.12233	0.49178	0.34493	0.991	Mg1-O4	2.19131
Mn2	0.12233	0.49178	0.34493	0.009	Mg1-O5	1.97006
Ge1	0.02835	0.3388	0.80419	1	Mg2-O1	2.04031
Ge2	0.22905	0.3454	0.0377	1	Mg2-O2	1.98739
O1	0.93678	0.33823	0.80115	1	Mg2-O3	2.35409

O2	0.07212	0.48479	0.67202	1	Mg2-O4	2.07033
O3	0.04831	0.32472	0.12636	1	Mg2-O5	2.05916
O4	0.31758	0.34117	0.00923	1	Mg2-O6	2.37165
O5	0.18544	0.51113	0.03178	1		
O6	0.19468	0.27513	0.32719	1		

Table S3 Fluorescence decay lifetimes of $M_{1-x}GOM_x$ (x = 1.0%, 1.5%, 2.0%, 2.5%, 3.0%, 3.5% and 4.0%) (λ_{ex}=260 nm, λ_{em}=679 nm).

Sample	A_1	τ_1 (ns)	A_2	τ_2 (ns)	R-square	τ^* (ms)
x=1.0%	1712.22833	2869116.40256	2926.68579	1.42209E7	0.99857	13.02
x=1.5%	1750.20694	2679180.6074	3000.2515	1.34358E7	0.99865	11,78
x=2.0%	1761.48557	2383762.53679	2980.86196	1.27743E7	0.99867	11,74
x=2.5%	1774.16551	2254861.94701	2946.02288	1.12774E7	0.99872	10.31
x=3.0%	1888.46163	1813844.09579	2857.80648	1.049E7	0.99865	9.60
x=3.5%	1937.32916	1498568.73388	2786.12222	9559481.06512	0.99849	8.77
x=4.0%	2009.89027	1095479.2125	2760.02117	8133180.19935	0.99831	7.51

The formation energy of a V_{Mg}'' defect in charge state q is defined the following equation[6]:

$$E^f[X^q] = E_{tot}[X^q] - E_{tot}[bulk] - \sum_i n_i\mu_i + qE_F + E_{corr}$$

$E_{tot}[X^q]$ is the total energy originated from a supercell calculation containing the defect V_{Mg}'', and $E_{tot}[bulk]$ is the total energy for the perfect crystal using an equivalent supercell. The integer n_i represents the number of atoms of type i (impurity atoms or host atoms) that have been added to ($n_i > 0$) or removed from ($n_i < 0$) the supercell to form the defect, and the μ_i is the corresponding chemical potentials of these species (chemical potentials display the energy of the reservoirs with which atoms are being exchanged). The analog of the chemical potential for "charge" is given by the chemical potential of the electrons, i.e., the Fermi energy E_F. Finally, E_{corr} is a correction term that accounts for finite k-point sampling in the case of shallow impurities, or for elastic

or electrostatic interactions between supercells. We present the charge state of a defect with a superscript q such as: for a neutral defect, q = 0; if one electron is removed, q = +1; if one electron is added, q = −1, etc. Interestingly, only neutral defects can occur in a metal. However, the defect can typically assume various charge states in a semiconductor or insulator, complected through exchanging electrons with an electron reservoir, which the energy is the electron chemical potential or Fermi level E_F, conventionally referenced to the VBM in the host.

Table S4 Total Energy (E_{tot}) and Formation Energy (E^f) of MGO for Mn^{4+} or Mn^{2+} ion doped.

MgGeO$_3$ compound	host	Mn^{2+} ion occupy Mg^{2+} site	Mn^{2+} ion replaces Mg^{2+} site leaving a $V_{Mg}^{''}$	Mn^{4+} ion replaces Mg^{2+} site leaving a $V_{Mg}^{''}$
E_{tot} (eV)	-4047.57	-4051.15	-4043.89	-4050.65
E^f (eV)	0	-2.87	-3.15	-3.86

Table S5 Fitted TL peaks and depth of traps energy level of $M_{1-x}GOM_x$ (x = 1.0%, 1.5%, 2.0%, 2.5%, 3.0%, 3.5% and 4.0%).

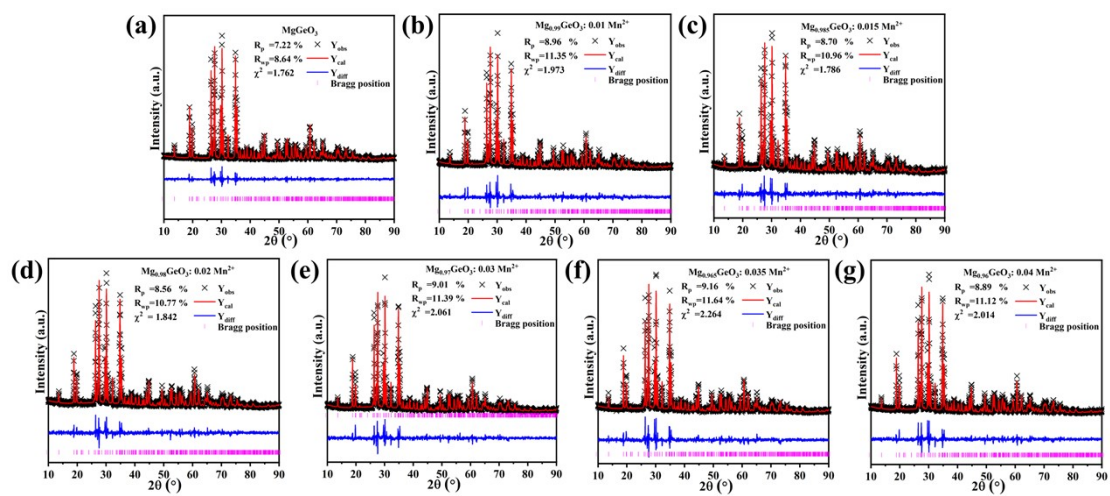| Sample	Peak 1 (K)	Peak 2 (K)	Peak 3 (K)	R-square	E1 (eV)	E2 (eV)	E3 (eV)
x=1.0%	365.0	430.9	505.5	0.99553	0.73	0.8618	1.011
x=1.5%	358.9	428.8	498.8	0.99427	0.7178	0.8576	0.9976
x=2.0%	359.5	424.1	490.5	0.99363	0.719	0.8482	0.981
x=2.5%	354.5	421.9	-	0.99662	0.709	0.8438	-
x=3.0%	356.7	421.6	-	0.99275	0.7134	0.8432	-
x=3.5%	359.9	428.7	-	0.994662	0.7198	0.8574	-
x=4.0%	353.8	418.1	-	0.99195	0.7076	0.8362	-

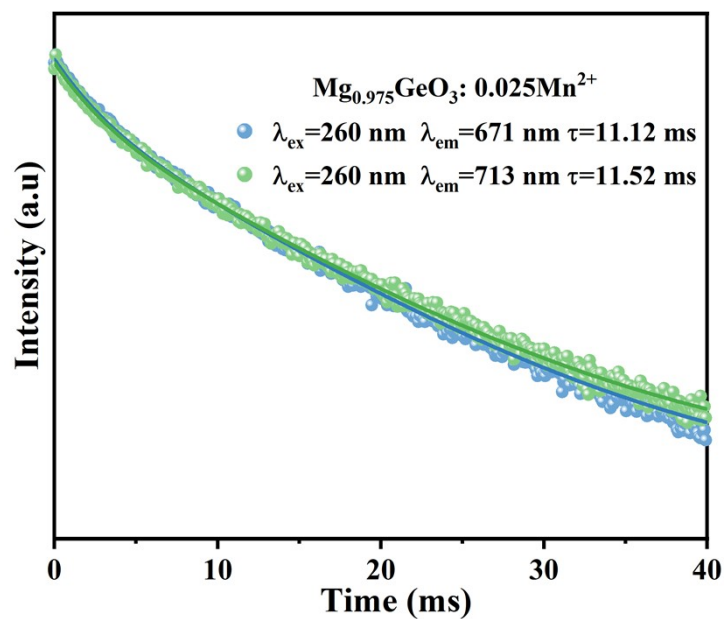**Figure S1** (a-g) Rietveld refinement results of $M_{1-x}GOM_x$ (x = 0.0%, 1.0%, 1.5%, 2.0%, 3.0%, 3.5% and 4.0%).

Figure S2 Fluorescence lifetime curves of $M_{0.975}GOM_{0.025}$ monitored at 671 and 713 nm, respectively, (λ_{ex}=260 nm).
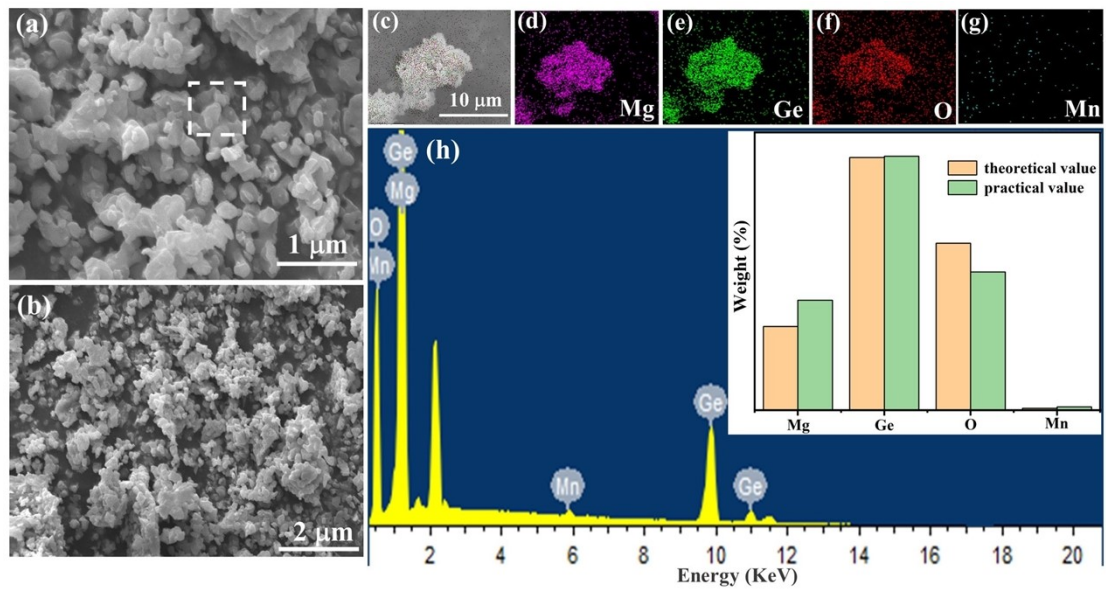
Figure S3 (a-b) SEM images of $M_{0.99}GOM_{0.01}$ at magnification of 10K (a) and 5K (b). (c) Selected area SEM image of $M_{0.99}GOM_{0.01}$. (d-g) The mapping images of elements Mg, Ge, O and Mn, respectively. (h) EDS elements analysis and a comparison of theoretical and practical value.
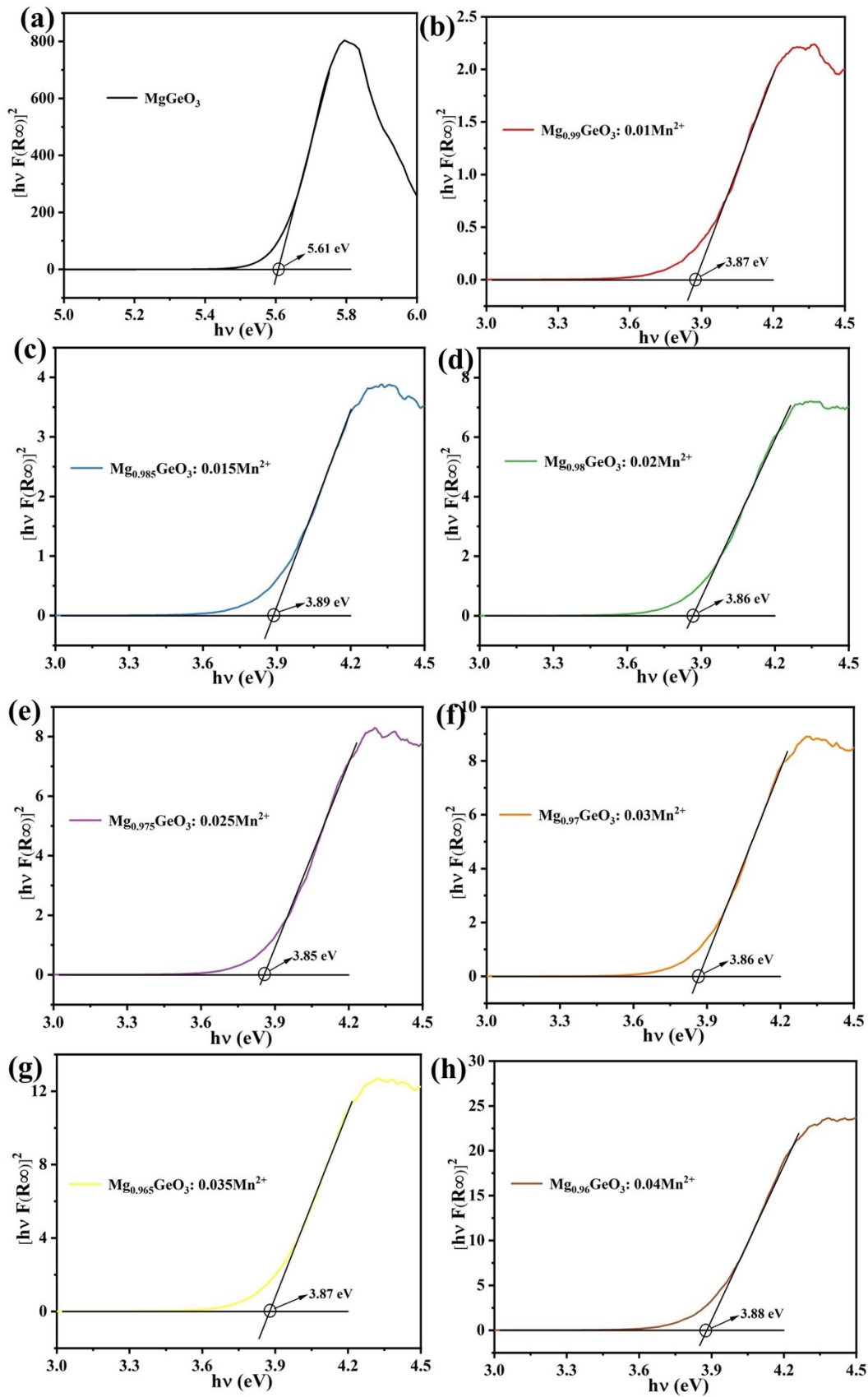
Figure S4 (a-h) Functional curve of $[hv\ F(\infty)]^2$ versus hv for calculation E_g value for $M_{1-x}GOM_x$ (x = 0.0%, 1.0%, 1.5%, 2.0%, 3.0%, 3.5% and 4.0%).
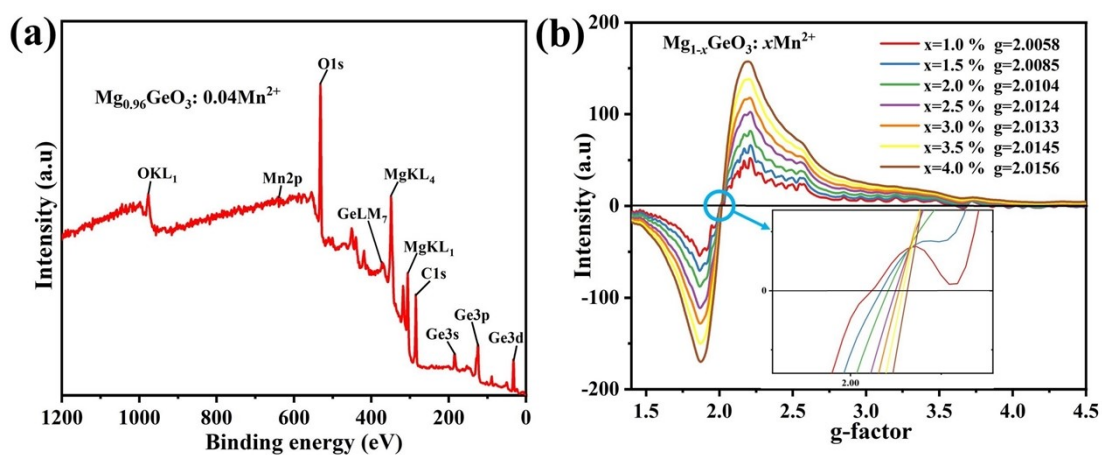
Figure S5 (a)XPS survey curve of $M_{0.96}GOM_{0.04}M$. (b) g-factor value of $M_{1-x}GOM_x$ (x = 1.0%, 1.5%, 2.0%, 3.0%, 3.5% and 4.0%). The inset shows enlarged curves.
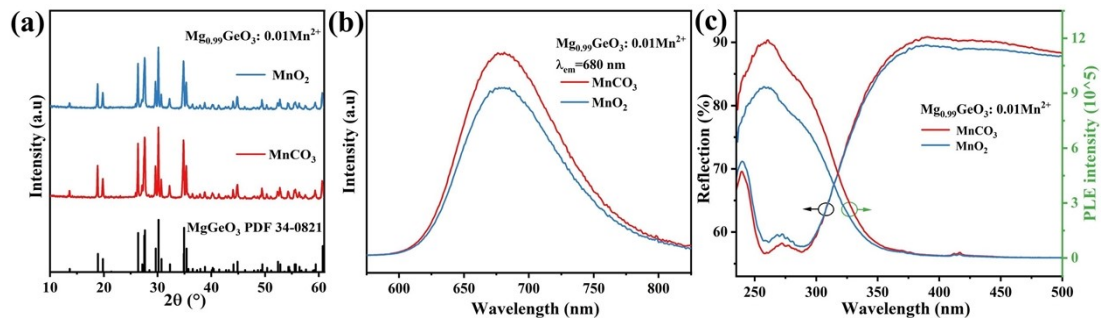
Figure S6 PL spectra of $M_{0.99}GOM_{0.01}$ using different manganese source ($MnCO_3$ and MnO_2, λ_{em}=680 nm). (b) XRD pattern of $M_{0.99}GOM_{0.01}$ using different manganese source ($MnCO_3$ and MnO_2). (c) PLE and DR spectra of $M_{0.99}GOM_{0.01}$ using different manganese source ($MnCO_3$ and MnO_2).
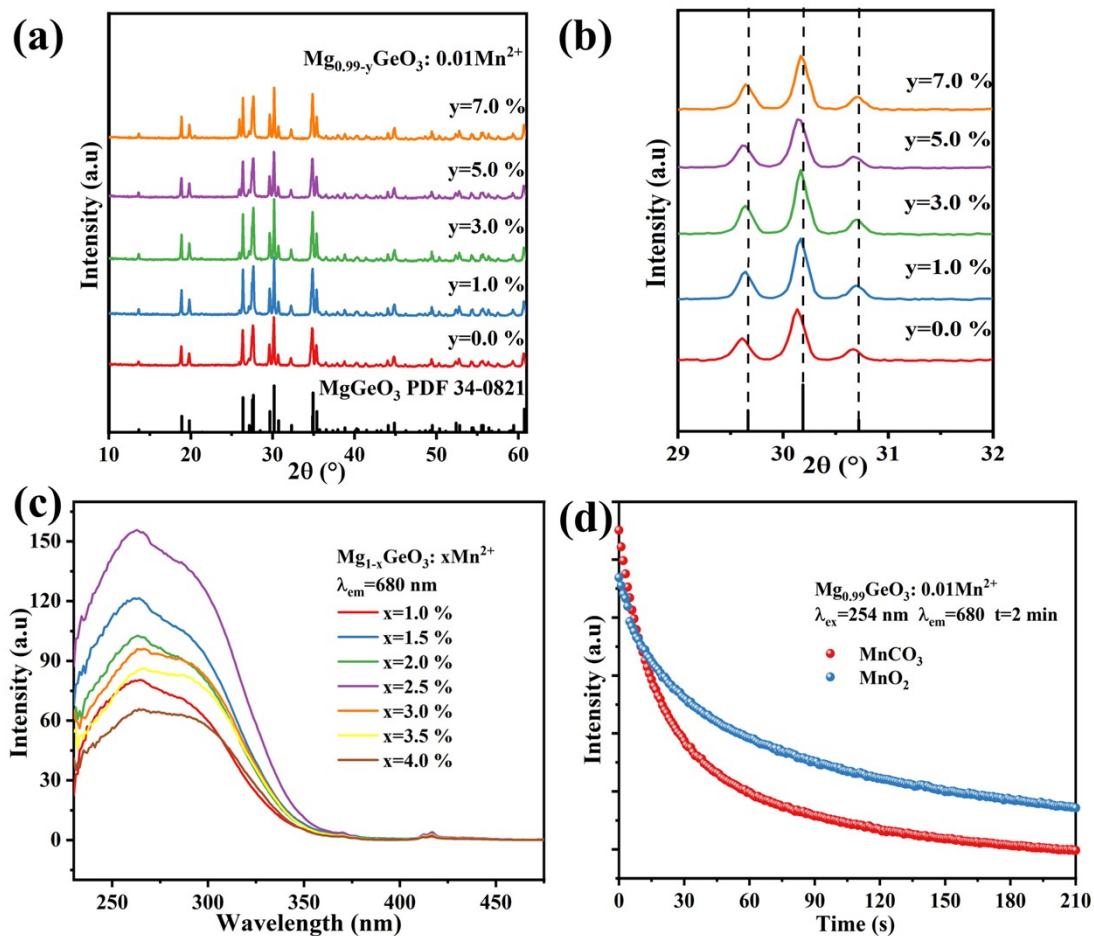
Figure S7 (a) XRD patterns of $M_{0.99-y}GOM_{0.01}$ (y = 0.0%, 1.0%, 3.0%, 5.0% and 7.0%) and the standard card of MGO (PDF 34-0821). (b) Partial enlargement of XRD pattern between 2θ = 29° and 32°. (c) PLE spectra of $M_{0.99-y}GOM_{0.01}$ (y = 0.0%, 1.0%, 3.0%, 5.0% and 7.0%). (d) PersL curves of $M_{0.99}GOM_{0.01}$ using different manganese source (MnCO$_3$ and MnO$_2$) (λ$_{ex}$=254 nm pre-irradiation 2 min, λ$_{em}$=679 nm).
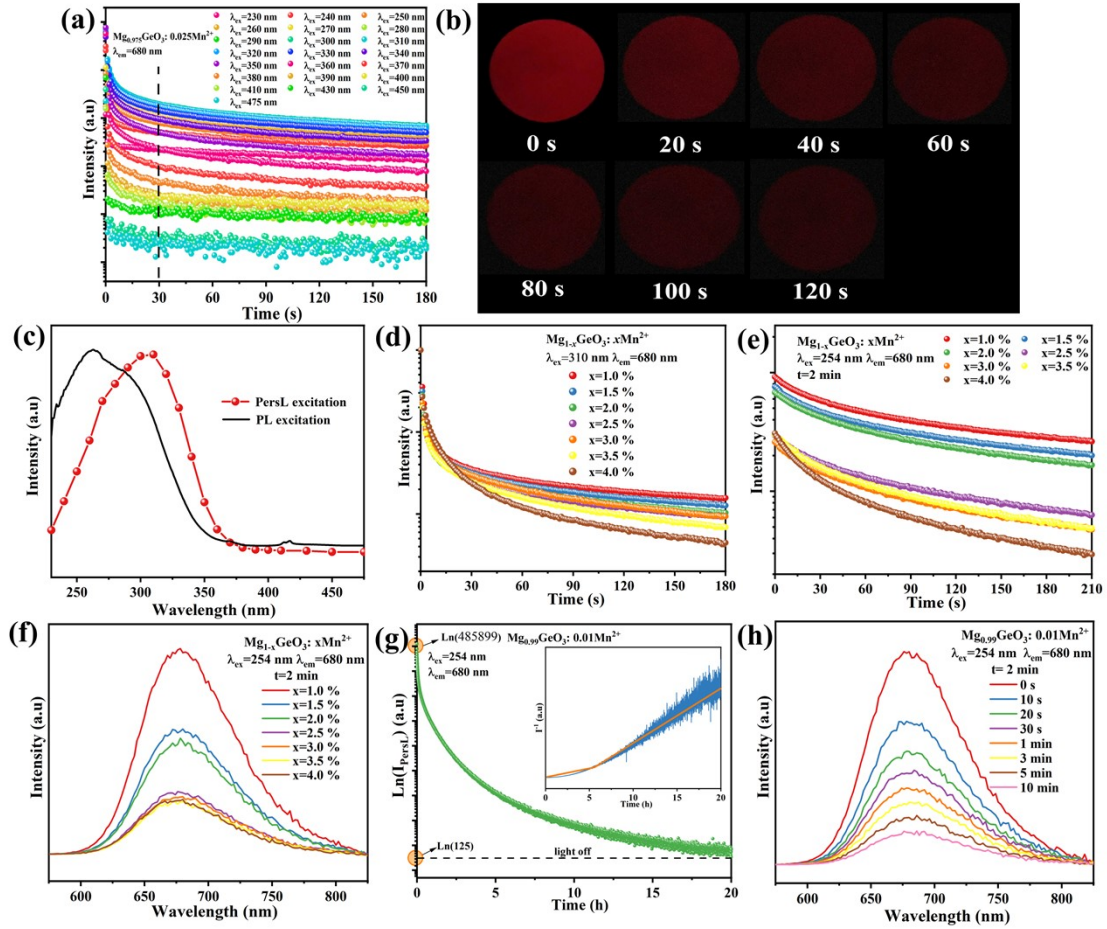
Figure S8 (a) PersL decay curves of $M_{0.975}GOM_{0.025}$ excited by different wavelength lights (Xe lamp, 230 nm-475 nm) for 30 s. (b) PersL images of $M_{0.99}GOM_{0.01}$ pre-irradiated by a 254 nm UV lamp for 2 min in 2 min decay. (c) PersL excitation spectra plotted by PersL intensity (recorded at 30 s delay) as a function of the excitation wavelength compared with PLE spectrum of $M_{0.975}GOM_{0.025}$. (d) PersL decay curves of $M_{1-x}GOM_x$ (x = 0.0%, 1.0%, 1.5%, 2.0%, 2.5%, 3.0%, 3.5% and 4.0%) (λ_{ex}=310 nm, λ_{em}=680 nm, Xe lamp). (e) PersL decay curves of $M_{1-x}GOM_x$ (x = 0.0%, 1.0%, 1.5%, 2.0%, 2.5%, 3.0%, 3.5% and 4.0%) (λ_{ex}=254 nm, λ_{em}=680 nm, UV lamp pre-irradiation for 2 min). (f) PersL spectra of $M_{1-x}GOM_x$ (x = 0.0%, 1.0%, 1.5%, 2.0%, 2.5%, 3.0%, 3.5% and 4.0%) (λ_{ex}=254 nm, UV lamp pre-irradiation for 2 min). (g) Ultra-PersL (15 h) curve of $M_{0.99}GOM_{0.01}$ and the reciprocal intensity (I^{-1}) versus time (t) (λ_{ex}=254 nm, λ_{em}=680 nm, UV lamp pre-irradiation for 2 min). (h) PersL spectra of $M_{0.99}GOM_{0.01}$ in 10 min decay （λ_{ex}=254 nm pre-irradiation for 2 min, λ_{em}=680 nm).
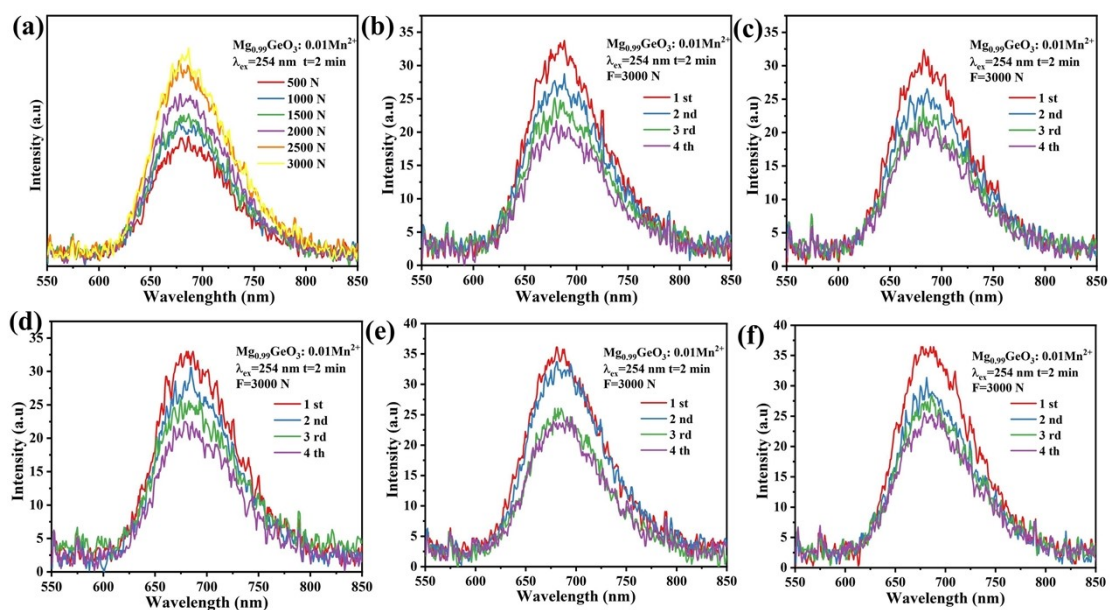
Figure S9 (a) ML spectra of $M_{0.99}GOM_{0.01}$ pre-irradiated by a 254 nm UV lamp for 2 min at different loading stresses (500, 1000, 1500, 2000, 2500 and 3000 N). (b-c) ML spectra of $M_{0.99}GOM_{0.01}$ recorded by four cycles at 40 s intervals (254 nm UV lamp pre-irradiation for 2 min at 3000 N cyclic loading stress) (b) 1st cycle; (c) 2nd cycle; (d) 3rd cycle; (e) 4th cycle; (f) 5th cycle.
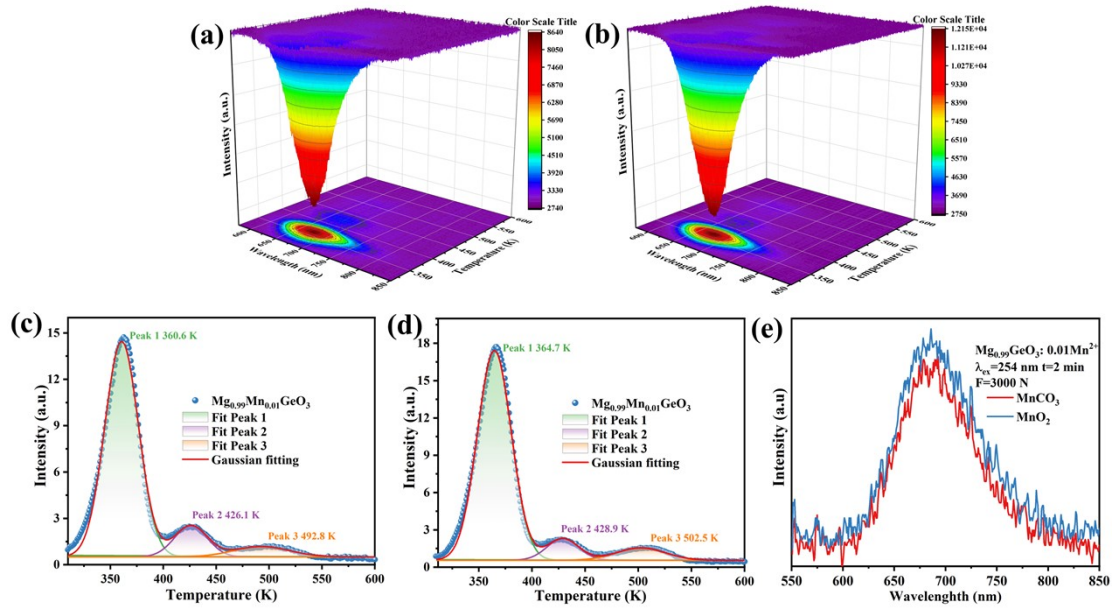
Figure S10 (a-b) Three-dimensional thermoluminescence of $M_{0.99}GOM_{0.01}$ using different manganese source of (a) $MnCO_3$ and (b) MnO_2. (c-d) Fitted TL curve of $M_{0.99}GOM_{0.01}$ using different manganese source of (c) $MnCO_3$ and (d) MnO_2. Green, purple, orange dotted line represented to Peak 1 (trap 1), Peak 2 (trap 2), and Peak 3 (trap 3), respectively. (e) ML spectra of $M_{0.99}GOM_{0.01}$ using different manganese source ($MnCO_3$ and MnO_2) pre-irradiated by a 254 nm UV lamp for 2 min at 3000 N loading.
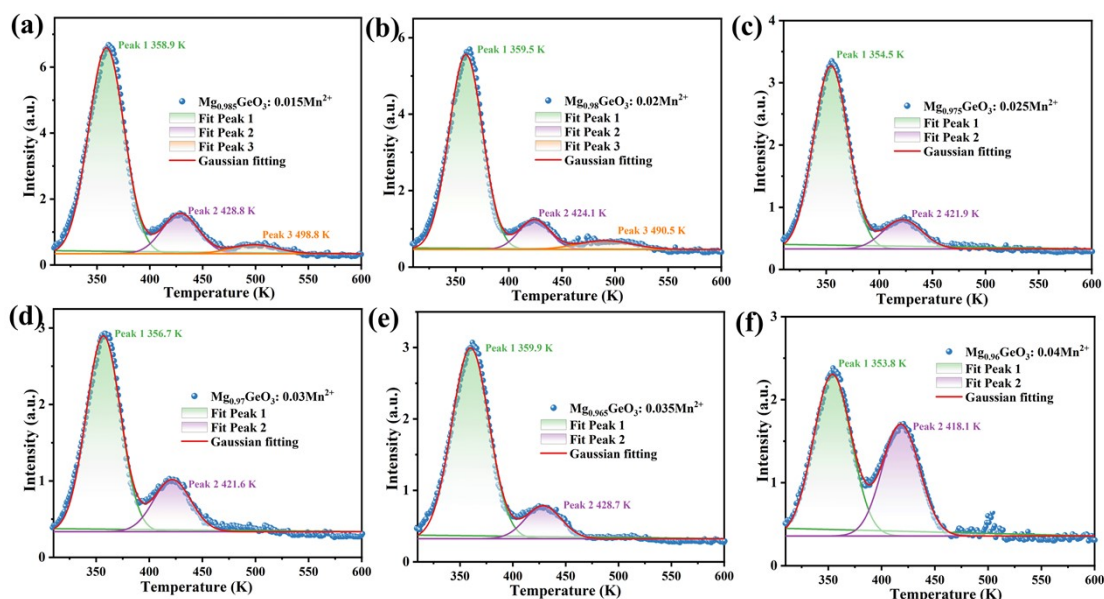
Figure S11 (a-f) Fitted TL curve of $M_{1-x}GOM_x$ (x = 1.5%, 2.0%, 2.5%, 3.0%, 3.5% and 4.0%); Green, purple, orange dotted line represented to Peak 1 (trap 1), Peak 2 (trap 2), and Peak 3 (trap 3), respectively.

References

1. S. Wu, Q. Liu, P. Xiong, W. Chen, Q. Dong, D. Chen, D. Wang, G. Zhang, Y. Chen and G. Li, *Adv. Opt. Mater.*, 2022, 2102842.

2. L. Guo, T. Wang, Q. Wang, W. Feng, Z. Li, S. Wang, P. Xia, F. Zhao and X. Yu, *Chem. Eng. J.*, 2022, **442**, 136236.

3. Y. Katayama, T. Kayumi, J. Ueda and S. Tanabe, *Opt. Mater.*, 2018, **79**, 147-151.

4. X. Ding, G. Zhu, W. Geng, Q. Wang and Y. Wang, *Inorg. Chem.*, 2016, **55**, 154-162.

5. F. Xiao, C. Xie, R. Yi, H. Yuan and Q. Zhou, *Opt. Mater.*, 2022, **125**, 112131.

6. C. Freysoldt, B. Grabowski, T. Hickel, J. Neugebauer, G. Kresse, A. Janotti and C. G. Van de Walle, *Rev. mod. phys.*, 2014, **86**, 253.